

# Biological Hotspots in the Galápagos Islands: Exploring Seasonal Trends of Ocean Climate Drivers to Monitor Algal Blooms

Emily Kislik, Gabriel Mantilla Saltos, Gladys Torres, Mercy Borbor-Córdova

**Abstract**—The Galápagos Marine Reserve (GMR) is an internationally-recognized region of consistent upwelling events, high productivity, and rich biodiversity. Despite its high-nutrient, low-chlorophyll condition, the archipelago has experienced phytoplankton blooms, especially in the western section between Isabela and Fernandina Islands. However, little is known about how climate variability will affect future phytoplankton standing stock in the Galápagos, and no consistent protocols currently exist to quantify phytoplankton biomass, identify species, or monitor for potential harmful algal blooms (HABs) within the archipelago. This analysis investigates physical, chemical, and biological oceanic variables that contribute to algal blooms within the GMR, using 4 km Aqua MODIS satellite imagery and 0.125-degree wind stress data from January 2003 to December 2016. Furthermore, this study analyzes chlorophyll-a concentrations at varying spatial scales—within the greater archipelago, as well as within five smaller bioregions based on species biodiversity in the GMR. Seasonal and interannual trend analyses, correlations, and hotspot identification were performed. Results demonstrate that chlorophyll-a is expressed in two seasons throughout the year in the GMR, most frequently in September and March, with a notable hotspot in the Elizabeth Bay bioregion. Interannual chlorophyll-a trend analyses revealed highest peaks in 2003, 2007, 2013, and 2016, and variables that correlate highly with chlorophyll-a include surface temperature and particulate organic carbon. This study recommends future in situ sampling locations for phytoplankton monitoring, including the Elizabeth Bay bioregion. Conclusions from this study contribute to the knowledge of oceanic drivers that catalyze primary productivity and consequently affect species biodiversity within the GMR. Additionally, this research can inform policy and decision-making strategies for species conservation and management within bioregions of the Galápagos.

**Keywords**—Bioregions, ecological monitoring, phytoplankton, remote sensing.

## I. INTRODUCTION

WITHIN the GMR in the eastern equatorial Pacific, consistent upwelling events support high productivity and a rich array of biodiverse marine species [1]-[3]. Although

the GMR is located within a region of high-nutrient, low-chlorophyll (HNLC) [1], previous studies have confirmed high productivity in the western GMR [1], [4]-[6]. In fact, waters surrounding the Galápagos host more than twice the phytoplankton biomass and primary production of any other equatorial upwelling region [7], thus providing the foundation for a complex marine food structure via trophic cascading [6], [8]-[10]. Furthermore, the Equatorial Undercurrent (EUC) supplies phytoplankton in this region with nutrients such as iron, nitrogen, phosphorus, and silicate [7], making the Elizabeth Bay bioregion home to the greatest density of endemic species in the archipelago [11]. However, climatic variability, which is expected to include greater severity of El Niño Southern Oscillation (ENSO) events and changes in upwelling and nutrient availability [12], will likely impact phytoplankton community structures, potentially resulting in declines that threaten food availability for higher trophic levels, or abundances that can produce HAB events [13]-[15]. The Instituto Oceanográfico de la Armada (INOCAR) and Instituto Nacional de Pesca (INP) have conducted several oceanographic research cruises west of Isabela and within the interior of several islands to study the structure of phytoplankton and zooplankton species and other variables in the Galápagos from the early 1970's [16] through the 2000's [17]-[21], yet oceanographic cruises do not sample these regions annually, and there is no scheduled monitoring system in place [14]. The lack of a consistent phytoplankton monitoring program in the archipelago results in sparse in situ data related to algal biomass quantification and species taxonomy in this region [22], [23]. Through analysis of remotely-sensed variables such as chlorophyll-a (Chla), a proxy for phytoplankton biomass [10], sea surface temperature (SST), an indicator of nutrient availability [24], and photosynthetically-available radiation (PAR), an indicator of light availability [25], it becomes possible to understand drivers that contribute to oceanic health within the GMR for future monitoring and management purposes.

The ocean climate system of the Galápagos is primarily affected by winds and ocean currents, which drive equatorial, coastal, and topographic upwelling within the GMR [2], [26]. Currents that flow around the archipelago include the warm Panama Current and North Equatorial Countercurrent in the north, the cold Peru and Humboldt Currents in the southeast, the South Equatorial Current that flows east to west through the center of the archipelago, and the cold Equatorial Undercurrent or Cromwell Current that moves from the west

E. Kislik is a Fulbright Fellow, visiting scientist at ESPOL, Guayaquil, Ecuador, and graduate student at the University of California, Berkeley (corresponding author, phone: 650-759-5419; e-mail: ekislik@berkeley.edu).

G. Mantilla Saltos is a researcher at ESPOL, Guayaquil, Ecuador (e-mail: gmantilla@espol.edu.ec).

G. Torres is with the Biology Department at the Instituto Oceanográfico de la Armada del Ecuador (INOCAR), Guayaquil, Ecuador (e-mail: gtorres@inocar.mil.ec).

M. Borbor-Córdova is a professor in the School of Naval Engineering, Oceanic, Biological Sciences and Natural Resources at the Escuela Superior Politécnica del Litoral (ESPOL), Guayaquil, Ecuador (e-mail: meborbor@espol.edu.ec).

to east, diverging around Isabela Island [1], [11], [22]. This latter subsurface current is the most significant physical oceanic process that contributes to elevated levels of local primary productivity in the western region of the archipelago [5], as it raises the thermocline in the east, supplies nutrients such as iron to the water column in the west, and increases Chla levels around Isabela Island [1], [6], [11], [24]. Understanding oceanic currents in the GMR, which directly affect upwelling and nutrient availability within this system [1], can provide insight into where potentially toxic microalgal species proliferate [27].

Little is known about how oceanographic dynamics affect biological production and phytoplankton populations in the archipelago [7], [24], and few studies have been published regarding phytoplanktonic species in the Galápagos [22]. This knowledge is necessary for understanding the risk of toxic blooms in this region. Of the studies conducted in the Galápagos, several species of potential HABs have been identified: *Mesodinium Rubrum* found in 1980, 1986, 2001, and 2009 in locations including north of Santa Cruz, south of Isabela, and in the Bolivar Channel [4], [28], [29], dinoflagellate cysts in coastal sediments in northern Caleta Tortuga Negra and southern Academy Bay of Santa Cruz

found in 1999 [22], *Ostreopsis* sp. south of Santa Cruz potentially linked to freshwater runoff found in 2007 [30], red tides about three to four times in the past 20 years observed at Punta Espinosa near Puerto Ayora [28], and a consistent red tide in Tortuga Bay in Santa Cruz, caused by the diatom *Bellerophon malleus* [29]. Also, *Pseudo-nitzschia delicatissima*, a diatom that can produce the neurotoxin domoic acid, and *Gymnodinium* sp., a dinoflagellate species that has been linked to paralytic shellfish poisoning [31], were found in Wreck Bay on San Cristóbal, Academy Bay on Santa Cruz, Puerto Velasco Ibarra Bay on Floreana, Puerto Villamil Bay on Isabela, and Darwin Bay on Genovesa in late 1999 [20]. *P. delicatissima* was found again more recently in the Bolivar Channel in March 2009 [4], and south of Isabela in September 2011 [32]. However, no official HABs have been reported in the archipelago thus far [33]. Due to the uncertainty of climatic variability, the risk of increasing toxic phytoplankton species in this system, and the inconsistency of current biological studies in this region, a basic monitoring program that includes sampling of SST and phytoplankton biomass would greatly benefit knowledge regarding the oceanic health of the Galápagos.

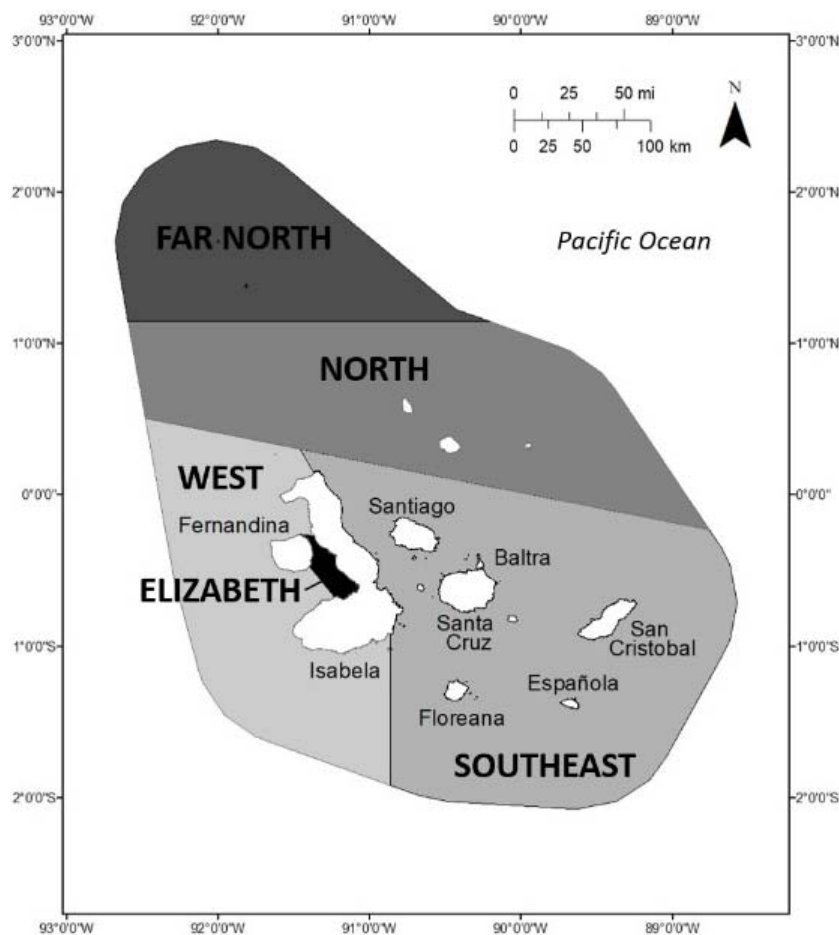


Fig. 1 Five bioregions of the GMR, as described by Edgar et al. [11]: Far North, North, Southeast, West, Elizabeth. Smaller text denotes the names of several islands in this archipelago

The purpose of this study is to investigate physical, chemical, and biological oceanic remotely-sensed variables that contribute to algal blooms within five bioregions of the GMR, explore seasonal and interannual trends of these variables, and use this information to identify future in situ sampling locations for phytoplankton monitoring within the Galápagos archipelago. Results from this research will aid environmental managers in the GMR in locating chlorophyll-a hotspots, reduce time and resources spent in the data collection process, assist in the application of a phytoplankton monitoring protocol, and promote greater awareness of how changes in phytoplankton communities affect GMR marine ecosystems.

## II. METHODOLOGY

### A. Study Area

This research utilized remotely-sensed imagery to analyze locations of high productivity within several biologically-diverse regions of the GMR. The GMR, located about 1000 km from the Ecuadorian mainland [11], [22], is the second-largest marine reserve in the world in area, following the Great Barrier Reef Marine Reserve [2], and is one of the most biologically diverse regions in the world [6].

There are two seasons on the islands: (1) the wet and hot season, from December to April, when the Intertropical Convergence Zone (ITCZ) moves south towards the equator, trade winds decrease, precipitation increases, and SSTs increase from a lack of Ekman divergence and increased evaporation, and (2) the dry or Garua season from May to November, when the ITCZ is north of the equator, trade winds increase, and SSTs diminish [24]. This information is critical in interpreting seasonal trends of climatic variability and productivity in the GMR.

To understand regions of high productivity, this study analyzed oceanic variables of the GMR, with special attention to five bioregions that delineate zones of similar species composition and biodiversity. These bioregions include: (1) Far North - Wolf and Darwin Islands, (2) North - Pinta, Marchena, Genovesa Islands, (3) Southeast - east of Isabela, (4) West - Fernandina and the western side of Isabela, and (5) Elizabeth - Elizabeth Bay and Bolivar Channel near Isabela (Fig. 1) [11].

### B. Remotely-Sensed Data

Six remotely-sensed variables in this study were utilized to create time series datasets, observe seasonal and interannual trends, and understand relationships among variables and chlorophyll-a abundance. Five 4-km Aqua MODIS products were obtained from the National Oceanic and Atmospheric Administration (NOAA) CoastWatch data server, ERDDAP, extracted using a bounding box (3N–3S, 93–88W), and subsequently constrained to the GMR. MODIS variables are global, monthly-averaged level 3 standard mapped image (SMI) products from January 2003 to December 2016, and include Chla, SST, PAR, particulate inorganic carbon (PIC), and particulate organic carbon (POC). Chla data serve as a

proxy for phytoplankton biomass [34], daytime 11-micron SST data were utilized to examine nutrient availability and the effects of upwelling and a shifting thermocline in the GMR [2], [24], [35], [36], and PAR data were used to estimate irradiance [25]. PIC describes estimations of calcium carbonate particles in the ocean, most of which are composed of by coccolithophores [37]. This variable is important because it represents the biomass of calcifying phytoplankton, and offers an estimation of potential carbon storage [38]. POC, which includes auto- and hetero-trophic microorganisms and detritus, is a measure of the production of phytoplankton photosynthesis [39], [40]. This variable is important because it is used to calculate phytoplankton growth, primary production, as well as potential oceanic carbon storage [39]. Also, this study incorporates a sixth variable, 0.125-degree (approximately 14 km at the equator) monthly-averaged wind stress (WS), to better understand an additional factor that contributes to upwelling [12], [41], [42]. WS data are products of the Quick Scatterometer (QuikSCAT) satellite from January 2003 to October 2009, and the Advanced Scatterometer (ASCAT) sensor on the EUMETSAT MetOp-A satellite from November 2009 to December 2016. These data were also acquired from NOAA's ERDDAP portal, and QuikSCAT imagery (0.25-degree resolution) was downsampled to 0.125 degrees to align with MetOp-A ASCAT data.

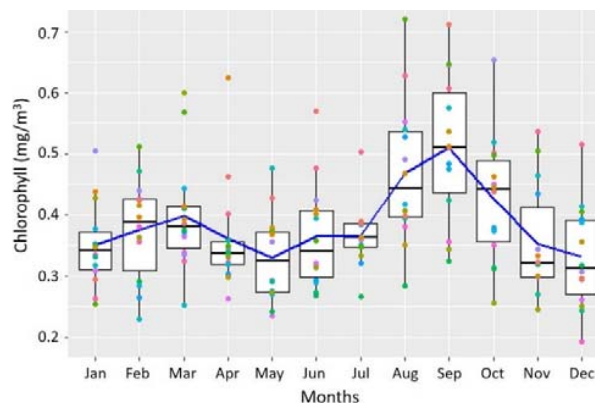


Fig. 2 Seasonal trend boxplot of monthly-averaged Aqua MODIS chlorophyll-a values from January 2003 to December 2016. The global monthly mean is depicted as the horizontal line

### C. Analyses

This study assessed seasonal and interannual trends, principal components, correlations among six variables, and Chla maxima within the GMR and specific bioregions. Analyses in this research included calculating global means and standard deviations per variable per month, characterizing variables by season (wet: December–April and dry: May–November) [24], creating a Principal Component Analysis (PCA) biplot [43] using six components [44], calculating correlations among all variables using Pearson's  $r$  [45], identifying Chla maxima values in the 75<sup>th</sup> and 90<sup>th</sup> percentiles of global mean values of the time series, and extracting values by bioregion. While extreme events are usually analyzed using data in the 90<sup>th</sup> percentile [46], this study also included values

in the 75<sup>th</sup> percentile to spatially visualize regions of high productivity that exist outside of the Elizabeth bioregion. Finally, interannual and extreme events were compared to NOAA's Climate Prediction Center Ocean Niño Index (ONI)

(Niño 3.4 region: 5N–5S, 120–170W). All analyses were performed in R Studio, using the packages Raster, NetCDF, GGCorrPlot, FactoMine, and Factoextra.

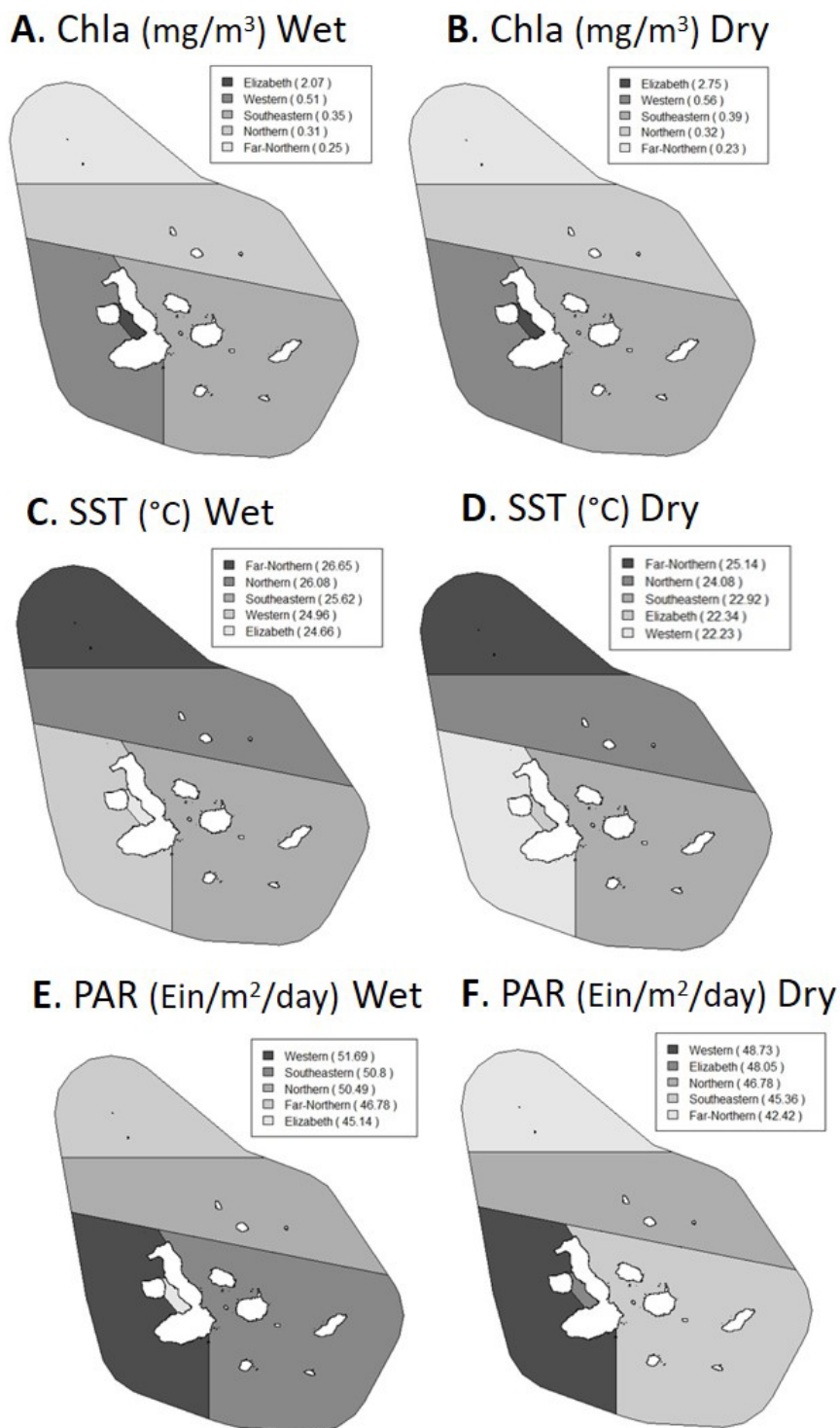


Fig. 3 Seasonally-averaged bioregion maps depicting (A) chlorophyll-a (mg/m<sup>3</sup>) in the wet season, (B) chlorophyll-a (mg/m<sup>3</sup>) in the dry season, (C) SST (°C) in the wet season, (D) SST (°C) in the dry season, (E) PAR (Einstein/m<sup>2</sup>/day) in the wet season, and (F) PAR (Einstein/m<sup>2</sup>/day) in the dry season. PIC, POC, and WS data were also calculated, but are not displayed in this study



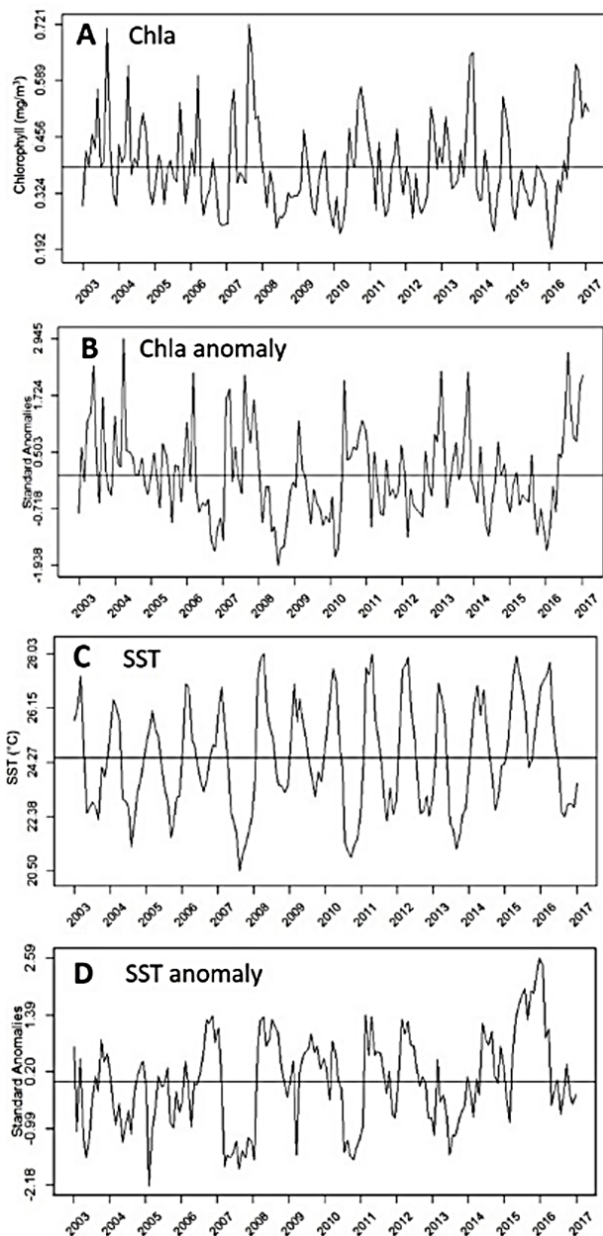


Fig. 4 Interannual trends from January 2003 to December 2016 of monthly (A) chlorophyll-a averages, (B) chlorophyll-a standard anomalies, (C) SST averages, and (D) SST standard anomalies. The horizontal line in each graph represents the global mean per dataset

### III. RESULTS

#### A. Seasonal Trends

Seasonal trend analyses of the GMR demonstrate that monthly Chla averages are expressed in two seasons throughout the year, with the highest peak in the month of September and a lower peak in March (Fig. 2). These results align with Chla seasonality observed 1-degree N in the GMR during a similar study conducted from 2002 to 2007 [6]. Monthly-averaged results also reveal that the lowest SST, highest PIC, highest POC, and highest WS events also

typically occur in the month of September, whereas the highest SST, highest PAR, and lowest WS events are most often observed in the month of March (Fig. 8).

Seasonal trend analyses of the bioregions demonstrate that the Elizabeth sector experienced the lowest SST ( $24.66^{\circ}\text{C}$ ) (Fig. 3 (C)) and PAR averages ( $45.14 \text{ Einstein/m}^2/\text{day}$ ) (Fig. 3 (E)) of all bioregions in the wet season, and highest Chla ( $2.75 \text{ mg/m}^3$ ) (Fig. 3 (B)), PIC ( $0.00017 \text{ mol/m}^3$ ) (data not shown), and POC ( $252.45 \text{ mg/m}^3$ ) (data not shown) averages throughout both seasons, with highest values in the dry season. The bioregion with the second-highest monthly-averaged Chla concentrations during both seasons is the Western region ( $0.56 \text{ mg/m}^3$  in dry season) (Fig. 3 (B)), due to the influence of the Elizabeth Bay region. The Western bioregion experienced the lowest SST in the dry season ( $22.23^{\circ}\text{C}$ ) (Fig. 3 (D)), and the highest PAR in both seasons, with highest PAR values in the wet season ( $51.69 \text{ Einstein/m}^2/\text{day}$ ) (Fig. 3 (E)). In contrast, the Far North bioregion experienced the lowest Chla ( $0.23 \text{ mg/m}^3$ ) (Fig. 3 (B)), PIC ( $4\text{e-}05 \text{ mol/m}^3$ ) (data not shown), and POC ( $66.51 \text{ POC mg/m}^3$ ) (data not shown) in both seasons, with lowest values in the dry season, as well as the lowest PAR averages of any bioregion in the dry season ( $42.42 \text{ Einstein/m}^2/\text{day}$ ) (Fig. 3 (F)). Additionally, the greatest values of seasonally-averaged WS ( $0.05 \text{ Pa}$  in the dry season) (data not shown) and SST ( $26.65^{\circ}\text{C}$  in the wet season) (Fig. 3 (C)) were observed in both seasons in the Far North bioregion. Due to the coarse resolution of the wind stress variable used in this study ( $0.125$  degrees), no WS data exists for the Elizabeth bioregion.

#### B. Climate Variability and Extreme Events

Analyses of the GMR show that the highest mean Chla peaks ( $>0.60 \text{ mg/m}^3$ ) occurred in 2007, 2003, 2013, 2016, 2004, and 2006, respectively (Fig. 4 (A)). The lowest mean SST peaks ( $<22.28^{\circ}\text{C}$ ) occurred in 2007, 2010, 2004, 2013, 2005, and 2003, respectively (Fig. 4 (C)). Thus, four of the six highest mean Chla peaks corresponded to years with the lowest mean SST events (2007, 2003, 2013, 2004). Finally, the highest overall monthly-averaged Chla event ( $0.72 \text{ mg/m}^3$ ) (Fig. 4 (A)) and lowest overall monthly-averaged SST event ( $20.50^{\circ}\text{C}$ ) (Fig. 4 (C)) were both observed in August 2007.

According to the Niño 3.4 region ONI, five El Niño and four La Niña events occurred throughout the study period. During the five El Niño events (June 2002–February 2003, July 2004–April 2005, September 2006–January 2007, July 2009–April 2010, November 2014–May 2016), Chla concentrations ranged from  $0.19$  to  $0.51 \text{ mg/m}^3$  (Fig. 4 (A)). During the four La Niña events (August 2007–June 2008, July 2010–April 2011, August 2011–February 2012, August 2016–December 2016), Chla concentrations ranged from  $0.24$  to  $0.72 \text{ mg/m}^3$  (Fig. 4 (A)). The highest Chla standard anomalies ( $>+2.19$ ) were observed in April 2004 ( $+2.94$ ), July 2016 ( $+2.64$ ), June 2003 ( $+2.36$ ), January 2003 ( $+2.24$ ), October 2013 ( $+2.22$ ), and March 2006 ( $+2.20$ ), respectively (Fig. 4 (B)). Aside from the second-highest Chla standard anomaly in July 2016, the five remaining largest positive Chla standard anomalies did not occur during La Niña events. Furthermore,

the second-highest Chla standard anomaly (+2.64) (Fig. 4 (B)) occurred six to eight months after the highest SST anomaly (+2.56) was observed in December 2015 (Fig. 4 (D)), during an extended El Niño event.

#### C. PCA and Correlations

The first two principal components explain 82.7% of the variability in the dataset (Fig. 5). The first component (51%) indicates that high monthly-averaged values of Chla, PIC,

POC, and WS are associated with the dry season, while the second component (31.7%) indicates that high SST and PAR values are associated with the wet season. Chla and PAR ( $r=0.003$ ) and Chla and WS ( $r=-0.07$ ) have negligible correlations throughout the GMR, while POC ( $r=0.94$ ), PIC ( $r=0.72$ ), and SST ( $r=-0.49$ ) have high correlations with Chla in the study area from January 2003 to December 2016 (Table I).

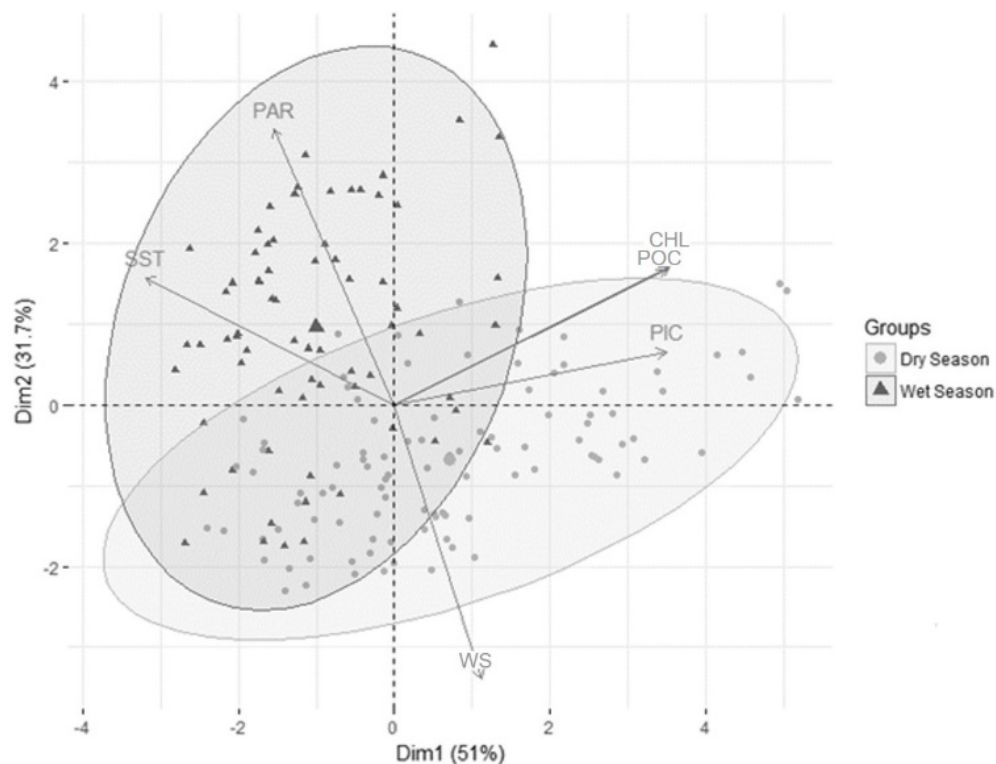


Fig. 5 Principal component analysis biplot depicting associations (components 1 and 2) among six variables during the wet and dry seasons

The Elizabeth bioregion expressed the highest correlation between PAR and Chla ( $r=0.41$ ) of all bioregions, and a relatively strong inverse relationship with SST ( $r=-0.39$ ) (Table I). The Western bioregion also displayed a relatively strong inverse relationship between Chla and SST ( $r=-0.39$ ), as well as the highest correlation between Chla and PIC of all bioregions ( $r=0.76$ ). The Far North bioregion exhibited the weakest correlation between Chla and SST ( $r=-0.06$ ), strongest correlation between Chla and WS ( $r=-0.39$ ), and highest correlation between Chla and POC ( $r=0.99$ ) of any bioregion. Overall, every bioregion had an inverse relationship between Chla and SST, Chla and WS (except for Elizabeth, due to lack of data), relatively strong positive correlation between Chla and PIC, and a near-1 correlation between Chla and POC. Correlations between PAR and Chla had the greatest variability among bioregions of all variables, resulting in a near-0 correlation within the GMR study region.

#### D. Chla Maxima

Regions with the highest Chla values throughout both seasons (mean pixel values in the 90<sup>th</sup> percentile or above, 0.50–11.13 Chla mg/m<sup>3</sup>) include Elizabeth Bay, the Bolivar Channel, and east of Isabela (Figs. 6 (A) and (B)). In addition to these locations, regions that express high Chla values throughout both seasons (mean pixel values in the 75<sup>th</sup> percentile or above, 0.38–11.13 Chla mg/m<sup>3</sup>) include the southern coast of Isabela, the northwestern coast of Santa Cruz, and the northern tip of Marchena (Figs. 6 (C) and (D)). During the wet season (December–April), northern San Cristóbal displays relatively high Chla concentrations, and during the dry season (May–November), the western coast of Santiago and west of Floreana exhibit relatively high productivity. Overall, bioregions of greatest productivity, based on monthly-averaged Chla data from January 2003 to December 2016, include Elizabeth (6.39 mg/m<sup>3</sup>), the West (4.79 mg/m<sup>3</sup>), and the Southeast (4.75 mg/m<sup>3</sup>) (Fig. 7).

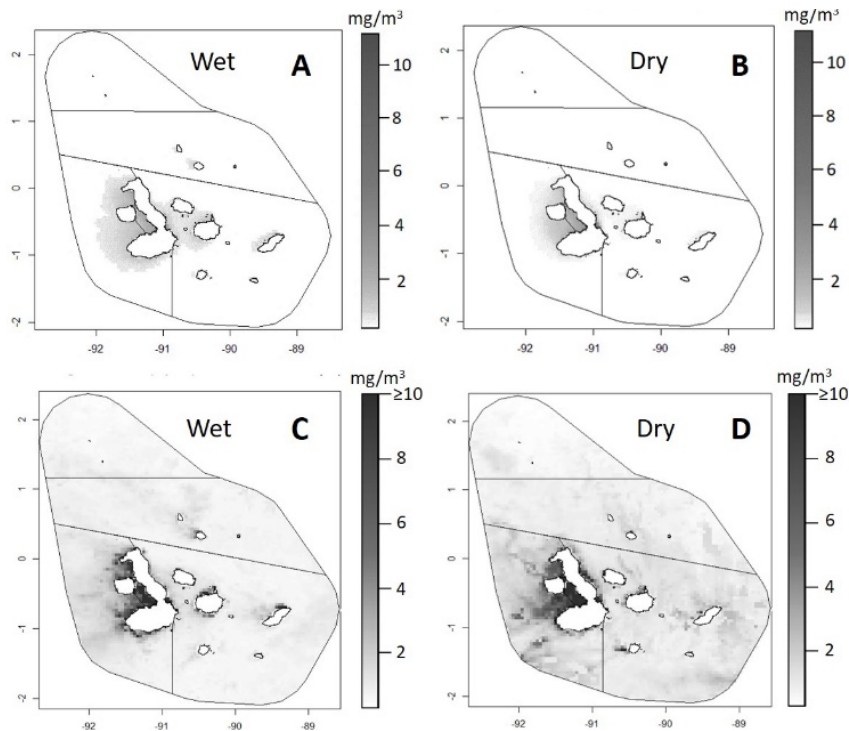


Fig. 6 Seasonally-averaged maximum chlorophyll-a ( $\text{mg}/\text{m}^3$ ) pixel values in the 90<sup>th</sup> percentile from January 2003 to December 2016 are represented by (A) the wet season, and (B) the dry season. Seasonally-averaged maximum chlorophyll-a ( $\text{mg}/\text{m}^3$ ) pixel values in the 75<sup>th</sup> percentile are represented by (C) the wet season, and (D) the dry season

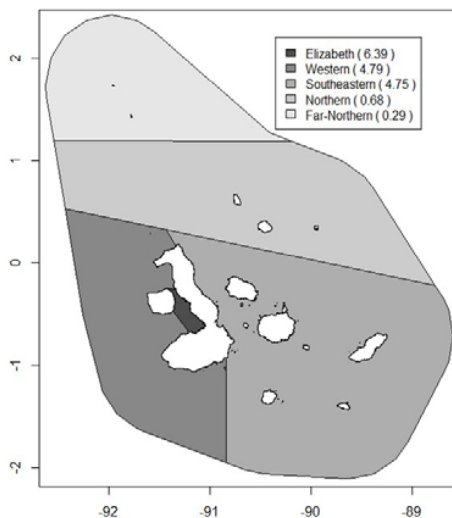


Fig. 7 Monthly-averaged maximum chlorophyll-a ( $\text{mg}/\text{m}^3$ ) pixel values in the 75<sup>th</sup> percentile, per bioregion, from January 2003 to December 2016

#### IV. DISCUSSION

##### A. Climate Variability and Extreme Events

Results from interannual trend analyses demonstrate that Niño 3.4 region events partially explain the variability of Chla concentrations observed throughout the GMR. Of the six greatest Chla standard anomalies, only the second-highest Chla standard anomaly coincided with a La Niña event.

Similarly, of the six lowest SST standard anomalies, only the very lowest SST standard anomaly of the time series coincided with an El Niño event. The Niño 3.4 region ONI does not capture all SST anomalies in the GMR from January 2003 to December 2016, yet SST anomalies and Chla anomalies in this study do demonstrate a large inverse relationship ( $r = -0.59$ ) (Fig. 9). Additionally, Chla anomalies observed in this research most often occurred between one to four months after SST anomalies occurred (Fig. 9). Although previous studies show that primary production typically increases during La Niña events [3], and Chla concentrations tend to decrease during El Niño events in the Galápagos [47], results from this study suggest that post-ENSO events may have a greater impact on Chla interannual variability. For example, the 2003 Chla anomaly may be explained by thermocline shoaling and a flow of iron from the New Guinea coastal undercurrent to the EUC; while this did not occur during a La Niña year, it followed the 2002 El Niño event [48]. Additionally, this study's second-highest Chla standard anomaly in July 2016 occurred between six to eight months after the highest SST standard anomalies were observed during the extended El Niño event from November 2014 to May 2016 (Figs. 4 (B) and (D)).

Generally, diminished Chla levels during El Niño events are attributed to warmer water masses that reduce surface nutrients and result in a phytoplankton compositional shift [36]. The transition from La Niña to El Niño conditions in the equatorial Pacific leads to an adjustment from diatom-dominated phytoplankton communities to cyanobacteria-

dominated populations [36], thus affecting base-line trophic levels. As diatoms have been observed to be the dominant phytoplankton group in 32 coastal oceanographic stations in the archipelago in late 1999 [20], in the Bolivar Channel in March 2009 [4], as well as in 12 locations within the GMR in September 2011 [32], more severe El Niño events might be implicated in reduced diatom dominance in these regions. While high Chla levels that follow in the wake of El Niño events suggest a shift from diatoms to more motile phytoplankton functional groups such as cyanobacteria or dinoflagellates [36], [49], additional research is needed to fully understand the complex dynamic between ENSO events and phytoplankton community ecological strategies during interannual transitions in the Galápagos.

#### *B. Currents and Upwelling Effects on Chla*

Although this research supports the conclusion that ENSO events contribute to altered chlorophyll-a levels in the GMR, analyses from this study suggest that nutrient availability from seasonal oceanic currents and upwelling events provide a more direct explanation for seasonal and interannual variability of Chla concentrations in this region. Three physical processes affect upwelling in the Galápagos: wind-driven equatorial upwelling across the archipelago, upwelling from the EUC on the west side of the islands, and topographically-driven upwelling on the coasts of the islands [2]. The EUC collides with the western side of the archipelago, Isabela Island, and upwelled surface waters are then transported to the eastern side of the islands via the South Equatorial Current [1], [24]. High Chla concentrations are also attributed to upwelling caused by subsurface topography, as high phytoplankton biomass has been observed over seamounts in the GMR where the EUC and South Equatorial Current converge [6].

Results from this study confirm the connection between high phytoplankton productivity in the western region and topographic upwelling from the EUC [7], as elevated Chla levels coincide with the annual seasonality of this system. The EUC is most prominent in the dry season, when upwelling is most pronounced, the thermocline is shallow [24], and seasonally-averaged chlorophyll-a levels in this study were the highest in all bioregions, especially in Elizabeth (2.57 mg/m<sup>3</sup>) and the West (0.56 mg/m<sup>3</sup>) (Fig. 3 (B)). During the wet season, when the EUC is reduced, the thermocline deepens, and upwelling decreases [24], the western archipelago experienced the greatest reduction in Chla levels (Elizabeth: -0.63 mg/m<sup>3</sup> change; Western: -0.05 mg/m<sup>3</sup> change) (Figs. 3 (A) and (B)). In contrast, the warm Panama Current and North Equatorial Countercurrent, which strengthen during the wet season [1], [11], contribute to the high SSTs (26.65°C) (Fig. 3 (C)) and low Chla levels (0.23 mg/m<sup>3</sup>) (Fig. 3 (B)) observed in the Far North bioregion between December and April. Finally, the GMR is located within a region that contributes the greatest amount of CO<sub>2</sub> to the atmosphere in the world; this is a result of equatorial upwelling [7]. Thus, additional analyses on how upwelling affects chlorophyll-a, and thus particulate organic carbon and particulate inorganic carbon, can enhance

understanding of carbon fluxes and potential storage in the GMR.

#### *C. Island Mass Effect*

Oceanic currents and upwelling events are not the only sources of nutrients for phytoplankton in the GMR; relatively high Chla concentrations that were observed in the absence of pronounced upwelling events can be partially attributed to the island mass effect (IME). This hypothesis encompasses several factors, including topographic upwelling, processes of oceanic mixing and vertical spreading, and nutrient supply from coastal sediments [1]. This effect has been found to increase chlorophyll-a concentrations around islands and atolls by over 85% above other oceanic conditions [10]. Due to a combination of cool upwelling in the western region, rocky subtidal reef ecosystems, and the presence of more than 100 islands and islets in the GMR [11], the Galápagos archipelago is a prime environment for the IME.

Although the eastern and central equatorial Pacific are regions of HNLC [1], the western GMR region expressed high monthly-averaged Chla pixel values during the wet season in this study (Chla  $\geq 10$  mg/m<sup>3</sup> in Elizabeth Bay and Bolivar Channel) (Figs. 6 (C) and (D)). This may be connected to iron provided by island sediments, as described by the IME [1], thus minimizing the effects of iron limitation in this otherwise HNLC region [50]. Hydrothermal vents in the western archipelago may also provide nutrients such as iron to phytoplankton communities [1]. Also, a combination of the IME and localized coastal upwelling likely explains the smaller Chla hotspots observed around Santa Cruz, Santiago, San Cristóbal, Floreana, and Marchena Islands (Figs. 6 (C) and (D)). Results from this study support the notion that the IME can significantly influence Chla concentrations around islands and atolls [10]. However, as information is limited on this topic in the GMR, further studies on the relationship between the IME and Chla concentrations in the Galápagos are recommended.

#### *D. Management Implications for Monitoring High Productivity in the GMR*

This study investigates seasonal trends of Chla concentrations as a proxy for phytoplankton activity and primary production, and identifies biological hotspots in Elizabeth Bay and the Bolivar Channel. However, there are many knowledge gaps in how climate-ocean drivers, vertical patterns linked to IME, and upwelled nutrients trigger high levels of productivity, as well as potential HABs. Thus, this study recommends the design and subsequent implementation of a long-term Ecological Monitoring Program of Phytoplankton (EMPP) to assess interannual variability of Chla concentrations in Elizabeth Bay, the Bolivar Channel, and other sites in the GMR. This program aims to increase knowledge on the drivers of algal growth, analyze effects of extreme climatic events on phytoplankton communities, and develop an early warning system for potentially toxic algal blooms and introduced HAB species.

The EMPP would be based on a collaborative framework of



stakeholders from scientific and marine resources management organizations, such as the Galápagos National Park (GNP), the Charles Darwin Foundation, INOCAR, INP, and residents or tourists who are interested in participating in citizen science. Data collection would involve an integrated approach that combines remote sensing and in situ sampling of phytoplankton species, including vertical profile measurements of variables such as Chla, SST, salinity, and dissolved oxygen [28], [51]. This program would serve as a mechanism to test monitoring protocols in localized regions, namely Elizabeth Bay and the Bolivar Channel, before applying best practices to other productive bioregions in the GMR.

The development of a Geographic Information System (GIS) platform that incorporates local algal bloom data and a map interface would benefit users such as researchers, marine managers, local authorities, and fishermen in the Galápagos. Finally, this monitoring program can provide information to agencies such as the Ministry of Public Health in the event of toxic algal blooms. Through the collaboration of local actors in the Galápagos, and a combination of data collection and database organization, the EMPP would help address conservation needs, assess climatic hazards, and analyze the status of oceanic health in the GMR.

#### V. CONCLUSIONS

This is the first study to analyze remotely-sensed variables that contribute to algal blooms in order to recommend future monitoring strategies within five bioregions of the GMR. Results from this research demonstrate that Chla concentrations express high variability across bioregions, exhibit bimodal seasonality, and are negatively correlated with

SST in the GMR. Additionally, elevated productivity observed in the Elizabeth and West bioregions is primarily attributed to a combination of nutrients supplied by the EUC, localized topographic upwelling, and iron provided by coastal sediments.

Predominant limitations of this study include distortions or lack of data from satellite imagery, resulting from factors such as coarse spatial, temporal, and spectral resolution, as well as clouds, aerosols, sunlight, solar zenith angle, and gaps in the imagery due to image capture and satellite orbit [36]. Furthermore, passive satellite imagery is unable to measure subsurface water properties such as chlorophyll maxima levels that are often found below 10 m depth [7], [34], [51]. Another limit of this study includes a lack of in situ data to validate satellite imagery and identify phytoplankton species. Therefore, there is a need to supplement remote sensing imagery with in situ data collection to gain a greater perspective on drivers of algal blooms within the GMR.

Results from this study can assist marine managers in making large-scale conservation and biodiversity decisions within the GMR, with the potential to positively impact critical habitats such as coral reefs [10] and species at risk of HAB exposure such as sea lions [33]. As great uncertainty exists in how the Galápagos marine environment will respond to climate variability [12], [26], it is important to continue deriving climatic information specific to bioregions within the Galápagos using in situ monitoring combined with time series analyses and oceanic modeling. This research utilizes remote sensing and geospatial analysis to understand seasonal trends of oceanic drivers in the GMR, and promotes the establishment of the EMPP that will benefit management strategies and oceanic health within this archipelago.

#### APPENDIX

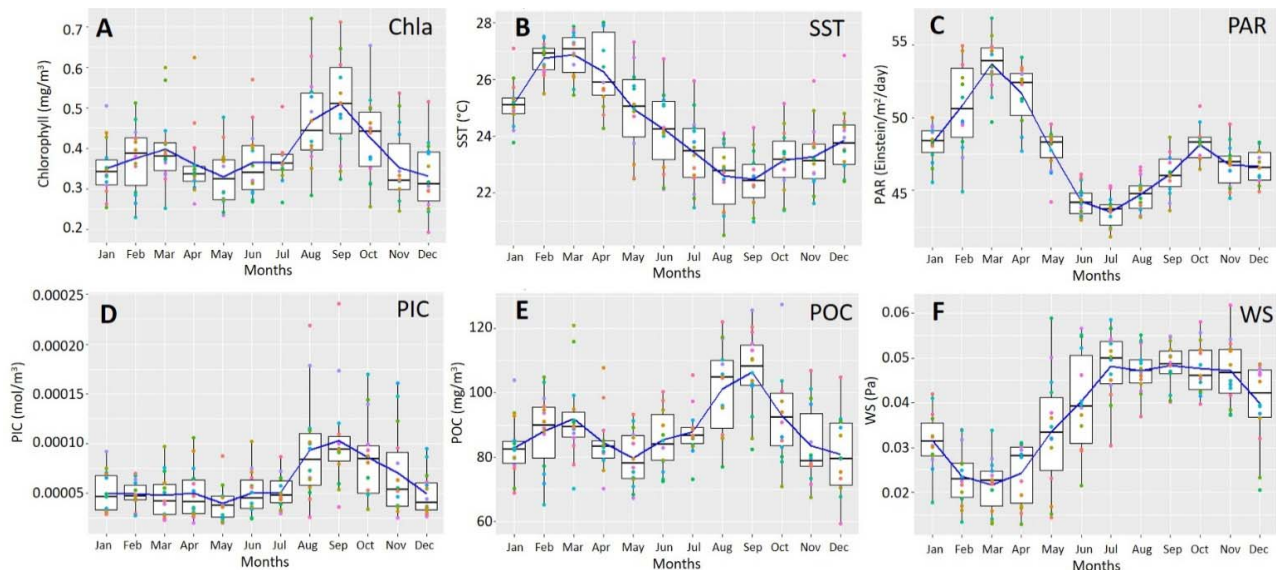


Fig. 8 Boxplots of monthly-averaged values of (A) Aqua MODIS chlorophyll-a, (B) Aqua MODIS SST, (C) Aqua MODIS photosynthetically-available radiation, (D) Aqua MODIS particulate inorganic carbon, (E) Aqua MODIS particulate organic carbon, (F) QuikSCAT and MetOp-A wind stress. Horizontal lines in each graph represent monthly global means

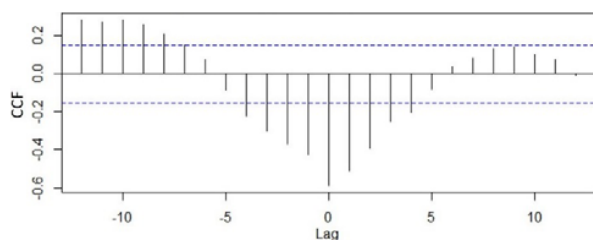


Fig. 9 Cross-correlations between SST standardized anomalies (independent variable) and Chla standardized anomalies (dependent variable) from January 2003 to December 2016. CCF on the y-axis signifies a unit of autocorrelation, and Lag on the x-axis signifies the monthly gap or delay between the two variables (one year in total is represented by this figure). Dotted horizontal lines represent limits of significance of 5% with respect to the CCF

TABLE I  
CORRELATIONS TO CHLOROPHYLL-A BY VARIABLE, PER REGION, FROM  
JANUARY 2003 TO DECEMBER 2016 USING PEARSON'S R. HIGH  
CORRELATIONS ( $R > 0.40$ ,  $R < -0.40$ ) ARE BOLDED.

Region	SST	PAR	PIC	POC	WS
Entire GMR	<b>-0.49</b>	0.003	<b>0.72</b>	<b>0.94</b>	-0.07
Elizabeth	-0.39	<b>0.41</b>	<b>0.44</b>	<b>0.91</b>	NA
Far North	-0.06	0.32	<b>0.46</b>	<b>0.99</b>	-0.39
North	-0.27	0.10	<b>0.73</b>	<b>0.98</b>	-0.13
Southeast	<b>-0.45</b>	-0.02	<b>0.68</b>	<b>0.98</b>	-0.05
West	-0.39	0.16	<b>0.76</b>	<b>0.91</b>	-0.16

#### ACKNOWLEDGMENT

The authors would like to thank members of the School of Naval Engineering, Oceanic, Biological Sciences and Natural Resources at the Escuela Superior Politécnica del Litoral (ESPOL) for invaluable research support. Additionally, the authors extend tremendous gratitude to Dr. Jose Marin, Nicolas Moity, and Ana Moya of the Charles Darwin Research Station, as well as Dr. Stuart Banks of Conservation International, for providing insight into several topics of this research. Financial Support comes from the Fulbright Commission of Ecuador and the Escuela Superior Politécnica del Litoral (ESPOL), Guayaquil, Ecuador.

#### REFERENCES

- [1] D. M. Palacios, "Factors influencing the island-mass effect of the Galápagos Archipelago," *Geophys. Res. Lett.*, vol. 29, no. 23, pp. 1–4, 2002.
- [2] J. Witman and F. Smith, "Rapid community change at a tropical upwelling site in the Galapagos Marine Reserve," *Biodivers. Conserv.*, vol. 12, pp. 25–45, 2003.
- [3] A. R. Longhurst, *Ecological Geography of the Sea*, 2nd ed. Academic Press, 2006.
- [4] C. Naranjo and M. E. Tapia, "Plancton en el canal bolívar de la isla isabela (caleta tagus), islas galápagos durante marzo de 2009," *Acta Ocean. del Pacífico*, vol. 20, no. 1, 2015.
- [5] J. Morrison, D. Kamykowski, L. Xie, S. Banks, and G. Feldman, "Biodiversity and Upwelling Dynamics of the Galapagos Marine Reserve," 2008.
- [6] B. A. Schaeffer *et al.*, "Phytoplankton biomass distribution and identification of productive habitats within the Galapagos Marine Reserve by MODIS, a surface acquisition system, and in-situ measurements," *Remote Sens. Environ.*, vol. 112, pp. 3044–3054, 2008.
- [7] J. T. Pennington, K. L. Mahoney, V. S. Kuwahara, D. D. Kolber, R. Calienes, and F. P. Chavez, "Primary production in the eastern tropical Pacific: A review," *Prog. Oceanogr.*, vol. 69, pp. 285–317, 2006.
- [8] Z. Lee, J. Marra, M. J. Perry, and M. Kahru, "Estimating oceanic primary productivity from ocean color remote sensing: A strategic assessment," *J. Mar. Syst.*, vol. 149, pp. 50–59, 2015.
- [9] V. Klemas, "Remote Sensing of Algal Blooms: An Overview with Case Studies," *J. Coast. Res.*, vol. 28, no. 1, pp. 34–43, 2012.
- [10] J. M. Gove *et al.*, "Near-island biological hotspots in barren ocean basins," *Nat. Commun.*, 2016.
- [11] G. J. Edgar, S. Banks, J. M. Fariña, M. Calvopiña, and C. Martinez, "Regional biogeography of shallow reef fish and macro-invertebrate communities in the Galapagos archipelago," *J. Biogeogr.*, vol. 31, no. 7, pp. 1107–1124, 2004.
- [12] J. P. Sachs and S. N. Ladd, "Climate and oceanography of the Galapagos in the 21st century: expected changes and research needs," *Galapagos Res.*, vol. 67, pp. 50–54, 2010.
- [13] T. Dickson, "A comparison of concentrations of macronutrients and chlorophyll a in high- and low- chlorophyll concentration areas around the Galápagos Islands Running head: Nutrient concentrations in the Galápagos Tamra Dickson University of Washington School of Ocea," University of Washington, 2006.
- [14] UNESCO, "Sexto Taller Regional de Planificación Científica sobre Floraciones de Algas Nocivas en Sudamérica," 2004.
- [15] D. Laffoley and J. M. Baxter, *Explaining Ocean Warming: Causes, scale, effects and consequences*, no. September. IUNC, 2016.
- [16] R. Jimenez, "Jiménez 1983 (cocolitofóridos en Ecuador).pdf," *Acta Ocean. del Pacífico*, vol. 2, no. 2, 1983.
- [17] M. L. García, G. Larrea, C. Aguirre, and A. Vásquez, "Zooplankto Biomass, Zooplankton and Ichthyoplankton Abundances around Galapagos Islands in 1983-1984," *Rev. Ciencias del Mar y Limnol.*, vol. 3, no. 1, pp. 17–18, 1993.
- [18] G. Torres and M. E. Tapia, "Distribución del primer nivel trófico (fitoplancton) en el Pacífico ecuatorial, periodo 1996-1997 (pre-El Niño)," *Acta Ocean. del Pacífico*, vol. 9, no. 1, 1998.
- [19] G. Torres and M. Tapia, "Distribución del fitoplancton y su comportamiento en el afloramiento en las islas Galápagos," *Acta Oceanográfica del Pacífico*, vol. 10, no. 1, pp. 137–150, 2000.
- [20] M. E. Tapia and G. Torres, "Variabilidad Fitoplanctonica en 5 Bahías, Islas Galapagos (Ecuador)," *Acta Ocean. del Pacífico*, vol. 10, no. 1, 2000.
- [21] G. Torres and M. E. Tapia, "Fitoplancton en el Afloramiento de las Islas Galápagos, durante agosto 2000," *Acta Ocean. del Pacífico*, vol. 11, no. 1, 2002.
- [22] K. Matsuoka, "Research Articles Modern Dinoflagellate Cysts Found in Surface," *Galapagos Res.*, vol. 63, no. June, pp. 8–11, 2005.
- [23] A. R. Fernández, "Coastal nutrient and water budget assessments for Puerto Ayora, Academy Bay, Santa Cruz Island," *The Significant Opportunities in Atmospheric Research and Science (SOARS) Program*. 2008.
- [24] W. V. Sweet, J. M. Morrison, D. Kamykowski, B. A. Schaeffer, S. Banks, and A. McCulloch, "Water mass seasonal variability in the Galapagos Archipelago," *Deep. Res. Part I Oceanogr. Res. Pap.*, vol. 54, pp. 2023–2035, 2007.
- [25] J. M. Gove *et al.*, "Quantifying Climatological Ranges and Anomalies for Pacific Coral Reef Ecosystems," *PLoS One*, vol. 8, no. 4, 2013.
- [26] M. Wolff, "Galápagos does not show recent warming but increased seasonality," *Galápagos Res.*, vol. 67, pp. 38–44, 2010.
- [27] R. Kudela, G. Pitcher, T. Probyn, F. Figueiras, T. Moita, and V. Trainer, "Harmful Algal Blooms in Coastal Upwelling Systems," *Oceanography*, vol. 18, no. 2, pp. 184–197, 2005.
- [28] G. Torres, "Eventos de Mareas Rojas: Estrategias de Gestión para el Manejo Integrado y Preventivo en Ecuador," Tesis para la obtención de Magister en Ciencias en Manejo Sustentable de Recursos Bioacuáticos y Medio Ambiente, Facultad de Ciencias Naturales de la Universidad de Guayaquil, 2012.
- [29] G. Torres, "Evaluación de mareas rojas durante 1968-2009 en Ecuador," *Acta Ocean. del Pacífico*, vol. 20, no. 1, 2015.
- [30] INOCAR, "Diagnóstico Ambiental de la Capitanía de Puerto Ayora Isla Santa Cruz," 2007. Unpublished.
- [31] C. Karaolis, "Effects of Global Warming on Harmful Algal Blooms Occurrence in the United States of America," Cyprus International Institute, 2004.
- [32] M. E. Tapia and C. Naranjo, "Aspectos oceanográficos del plancton y su relación con el Frente Ecuatorial, durante septiembre de 2011," *Acta Ocean. del Pacífico*, vol. 17, no. 1, 2012.
- [33] J. Denkinger *et al.*, "Pup Mortality and Evidence for Pathogen Exposure in Galapagos Sea Lions (*Zalophus Wollweberi*) on San

- Cristobal Island, Galapagos, Ecuador," *J. Wildl. Dis.*, vol. 53, no. 3, pp. 491–498, 2017.
- [34] D. Blondeau-Patissier, J. F. R. Gower, A. G. Dekker, S. R. Phinn, and V. E. Brando, "A review of ocean color remote sensing methods and statistical techniques for the detection, mapping and analysis of phytoplankton blooms in coastal and open oceans," *Prog. Oceanogr.*, vol. 123, pp. 123–144, 2014.
- [35] P. A. Diaz *et al.*, "Climate variability and oceanographic settings associated with interannual variability in the initiation of dinophysis acuminata blooms," *Mar. Drugs*, vol. 11, no. 8, pp. 2964–2981, 2013.
- [36] C. S. Rousseaux and W. W. Gregg, "Interannual variation in phytoplankton primary production at a global scale," *Remote Sens.*, vol. 6, no. 1, pp. 1–19, 2014.
- [37] W. M. Balch, D. T. Drapeau, T. L. Cucci, R. D. Vaillancourt, K. a. Kilpatrick, and J. J. Fritz, "Optical backscattering by calcifying algae: Separating the contribution of particulate inorganic and organic carbon fractions," *J. Geophys. Res.*, vol. 104, no. C1, p. 1541, 1999.
- [38] W. M. Balch, D. T. Drapeau, J. J. Fritz, B. C. Bowler, and J. Nolan, "Optical backscattering in the Arabian Sea - Continuous underway measurements of particulate inorganic and organic carbon," *Deep. Res. Part I Oceanogr. Res. Pap.*, vol. 48, no. 11, pp. 2423–2452, 2001.
- [39] D. Stramski *et al.*, "Relationships between the surface concentration of particulate organic carbon and optical properties in the eastern South Pacific and eastern Atlantic Oceans," *Biogeosciences*, vol. 5, no. 1, pp. 171–201, 2008.
- [40] D. Liu *et al.*, "Remote sensing observation of particulate organic carbon in the Pearl River Estuary," *Remote Sens.*, vol. 7, pp. 8683–8704, 2015.
- [41] J. Kämpf and P. Chapman, *Upwelling systems of the world: A scientific journey to the most productive marine ecosystems*. 2016.
- [42] M. Kahru *et al.*, "Global correlations between winds and ocean chlorophyll," *J. Geophys. Res. Ocean.*, vol. 115, no. 12, pp. 1–11, 2010.
- [43] A. Kassambara and F. Mundt, "Package 'factoextra,'" *R topics documented*. p. 75, 2017.
- [44] I. T. Jolliffe, "Principal Component Analysis, Second Edition," *Encycl. Stat. Behav. Sci.*, vol. 30, no. 3, p. 487, 2002.
- [45] K. Pearson, "On lines and planes of closest fit to systems of points in space," *Philos. Mag. J. Sci.*, vol. 2, no. 1, pp. 559–572, 1901.
- [46] A. M. Grimm and R. G. Tedeschi, "ENSO and extreme rainfall events in South America," *J. Clim.*, vol. 22, pp. 1589–1609, 2009.
- [47] M. Wolff, D. J. Ruiz, and M. Taylor, "El Niño induced changes to the Bolivar Channel ecosystem (Galapagos): comparing model simulations with historical biomass time series," *Mar. Ecol. Prog. Ser.*, vol. 448, pp. 7–22, 2012.
- [48] J. P. Ryan, I. Ueki, Y. Chao, H. Zhang, P. S. Polito, and F. P. Chavez, "Western Pacific modulation of large phytoplankton blooms in the central and eastern equatorial Pacific," *J. Geophys. Res. Biogeosciences*, vol. 111, pp. 1–14, 2006.
- [49] P. W. Glynn, "Global Ecological Consequences of the 1982-83 El Niño-Southern Oscillation," *Mar. Biol. Fish.*, vol. 52, no. 1, 1990.
- [50] D. M. Palacios, "Seasonal patterns of sea-surface temperature and ocean color around the Galapagos: regional and local influences," *Deep. Res. II*, vol. 51, pp. 43–57, 2004.
- [51] G. Torres, "Areas de mayor productividad biologica (clorofila a) en el pacifico ecuatorial (82°W-92°W) durante 1988-1999 y su relacion con eventos del niño," *Acta Ocean. del Pacífico*, vol. 13, no. 1, 2006.